

Title	Resonance assisted jump-in voltage reduction for electrostatically actuated nanobeam-based gateless NEM switches.
Authors	Meija, Raimonds;Livshits, Alexander I.;Kosmaca, Jelena;Jasulaneca, Liga;Andzane, Jana;Biswas, Subhajit;Holmes, Justin D.;Erts, Donats
Publication date	2019-07-08
Original Citation	Meija, R., Livshits, A. I., Kosmaca, J., Jasulaneca, L., Andzane, J., Biswas, S., Holmes, J. D. and Erts, D. (2019) 'Resonance assisted jump-in voltage reduction for electrostatically actuated nanobeam-based gateless NEM switches', Nanotechnology, 30(38), 385203 (6 pp). doi: 10.1088/1361-6528/ab2b11
Type of publication	Article (peer-reviewed)
Link to publisher's version	https://iopscience.iop.org/article/10.1088/1361-6528/ab2b11 - 10.1088/1361-6528/ab2b11
Rights	© 2019 IOP Publishing Ltd. This is an author-created, un-copyedited version of an article accepted for publication in Nanotechnology The publisher is not responsible for any errors or omissions in this version of the manuscript or any version derived from it. The Version of Record is available online at https://doi.org/10.1088/1361-6528/ab2b11 . As the Version of Record of this article has been published on a subscription basis, this Accepted Manuscript will be available for reuse under a CC BY-NC-ND 3.0 licence after a 12 month embargo period. - https://creativecommons.org/licences/by-nc-nd/3.0
Download date	2024-05-16 18:26:55
Item downloaded from	https://hdl.handle.net/10468/8213



University College Cork, Ireland
Coláiste na hOllscoile Corcaigh

ACCEPTED MANUSCRIPT

Resonance assisted jump-in voltage reduction for electrostatically actuated nanobeam-based gateless NEM switches

To cite this article before publication: Raimonds Meija *et al* 2019 *Nanotechnology* in press <https://doi.org/10.1088/1361-6528/ab2b11>

Manuscript version: Accepted Manuscript

Accepted Manuscript is "the version of the article accepted for publication including all changes made as a result of the peer review process, and which may also include the addition to the article by IOP Publishing of a header, an article ID, a cover sheet and/or an 'Accepted Manuscript' watermark, but excluding any other editing, typesetting or other changes made by IOP Publishing and/or its licensors"

This Accepted Manuscript is © 2019 IOP Publishing Ltd.

During the embargo period (the 12 month period from the publication of the Version of Record of this article), the Accepted Manuscript is fully protected by copyright and cannot be reused or reposted elsewhere.

As the Version of Record of this article is going to be / has been published on a subscription basis, this Accepted Manuscript is available for reuse under a CC BY-NC-ND 3.0 licence after the 12 month embargo period.

After the embargo period, everyone is permitted to use copy and redistribute this article for non-commercial purposes only, provided that they adhere to all the terms of the licence <https://creativecommons.org/licences/by-nc-nd/3.0>

Although reasonable endeavours have been taken to obtain all necessary permissions from third parties to include their copyrighted content within this article, their full citation and copyright line may not be present in this Accepted Manuscript version. Before using any content from this article, please refer to the Version of Record on IOPscience once published for full citation and copyright details, as permissions will likely be required. All third party content is fully copyright protected, unless specifically stated otherwise in the figure caption in the Version of Record.

View the [article online](#) for updates and enhancements.

**Resonance assisted jump-in voltage reduction for electrostatically actuated
nanobeam-based gateless NEM switches**

Meija R.¹, Livshits A.I. ¹, Kosmaca J. ¹, Jasulaneca L. ¹, Andzane J. ¹, Biswas S. ², Holmes²
J.D., Erts D^{1,3}.

¹Institute of Chemical Physics, University of Latvia

²School of Chemistry, ERI and the Tyndall National Institute, University College Cork, Cork, Ireland

³Faculty of Chemistry, University of Latvia

Abstract

Electrostatically actuated nanobeam-based electromechanical switches have shown promise for versatile novel applications, such as low power devices. However, their widespread use is restricted due to poor reliability resulting from high jump-in voltages. This article reports a new method for lowering the jump-in voltage by inducing mechanical oscillations in the active element during the switching ON process, reducing the jump-in voltage by more than 3 times. $\text{Ge}_{0.91}\text{Sn}_{0.09}$ alloy and Bi_2Se_3 nanowire-based nanoelectromechanical switches were constructed *in-situ* to demonstrate the operation principles and advantages of the proposed method.

Introduction

Nanoelectromechanical (NEM) systems have shown great promise in the automotive [1], space [2] and electronics [3] industries for applications such as high frequency resonators [4], mass sensing [5–7] and switches [8–12]. NEM systems represent the next technological advancement after microelectromechanical (MEM) systems in terms of switching speed, energy efficiency and integration density.

A NEM switch is a type of a NEM system, where mechanical and electrical properties of flexible nanostructures are exploited for switching between the ON and OFF positions. NEM switches have been proposed as low power [13] devices with small leakage currents and high on/off ratios [14–17]. Currently, the biggest challenge that delays the commercialization of NEM switches, especially proposed gateless switches with high jump-in voltages, is their insufficient durability [11,12].

One of the main challenges for the durable operation of a gate-less NEM switch is controlling electric field induced effects. Uncontrolled, these effects may result in the permanent ON state (stiction) or burn-out of the flexible element of the switch. High electric fields, in the order of 10^8 V/m, between the contact electrodes may result in switch stiction due to the field-induced material transfer [18,19]. For metal-metal nanocontacts, the material transfer induced stiction has been reported for the source-drain voltage exceeding 5 V [19]. Higher jump-in voltages can also result in electric field induced burn-out of the flexible element in two-terminal devices [8,10,20–22]. Low jump-in voltages for a particular switch architecture will therefore likely increase the durability of a switch.

Several approaches to lower the jump-in voltage for gate-less switches have been reported, with the most straightforward method being a reduction of the separation gap between the flexile element and the contact electrode [17,23]. A drawback of this approach is a decrease of the restoring elastic force accompanying the separation gap reduction, often resulting in a permanent stiction of the flexile element in an ON state due to the adhesion in the contact with the electrode. Other more sophisticated ways to lower the jump-in voltage have included using novel device architectures, e.g., pipe-clip design [15], and operating the switch in a dielectric liquid [24].

The flexile elements of NEM switches are either fabricated by top-down processes, using e-beam lithography techniques, or synthesized independently by a bottom-up technique and then arranged to the desired positions on the NEM device during its configuration. Using synthesized nanowires instead of lithography made nanobeams as flexile elements in the NEM switches offers increased control over their chemical composition and morphology. Other advantages include smooth contact surfaces, low defect densities and mechanical properties that approach the theoretical limits for strength [25].

We have previously shown that mechanical oscillations of a flexile element can be utilized to monitor switch dynamics and adjust contact adhesion between an electrode and the flexile element in a NEM switch [26,27]. We have also reported a method for switching a nanowire flexile element in a NEM device from an ON to OFF state by inducing resonant mechanical oscillations [28], reducing the work of adhesion and consequently the switching voltage by up to 10 times for the gate-less

1
2
3 NEM switches. Oscillations induced in the flexile element have also been used to
4
5 monitor its mechanical strain [27] and the changes in NEM switch nanocontacts [29].
6
7

8
9 This article reports a novel approach to decrease the jump-in voltage (ON state) by
10
11 inducing electrostatically induced mechanical oscillations in the flexile element of a
12
13 NEM switch while it is in its OFF state. The method allows maintenance of a large
14
15 initial separation gap between the flexile element and the contact electrode, leading
16
17 to an elastic restoration force strong enough to overcome adhesion in the ON state
18
19 contact. This approach also limits the jump-in current, thus preventing current-
20
21 induced modifications in the contact during the ON state, which could result in a
22
23 permanent stiction of the switch [17,23,29]. This method is presented for both
24
25 cylindrical $\text{Ge}_{0.91}\text{Sn}_{0.09}$ (GeSn) and rectangular Bi_2Se_3 nanowires. We chose GeSn
26
27 nanowires, because of their combination of high mechanical strength [30], lower
28
29 resistivity [31] and absence of non-conductive germanium oxide outer shell [32] that
30
31 is present in previously used Ge nanowires [8]. Bi_2Se_3 nanowires were chosen
32
33 because of their lower resistivity and increased contact area due to their rectangular
34
35 shape, thus making them more conductive [33,34]. As Bi_2Se_3 is a thermoelectric
36
37 material [35], they could be also used in novel applications, for example, to detect
38
39 temperature difference across switch terminals.
40
41
42
43
44
45
46
47
48
49
50

51 **Materials and methods**

52
53
54 The experiments were carried out *in-situ* SEM Hitachi S-4800. For the contact
55
56 electrodes, electrochemically etched gold (GoodFellow 99.95 %) tips were used.
57
58
59 Sharp tips were used to achieve a smaller contact area and thus lower adhesion in
60

the contact. A SmarAct 13D nanomanipulator was used to transfer nanowires from substrates used for their synthesis to gold tips, and for acquiring the desired switch geometry.

GeSn and Bi₂Se₃ nanowires (cylindrical and rectangular shapes) were used as switching elements. The GeSn nanowires were synthesized by a vapor-liquid-solid method [32] and the Bi₂Se₃ nanowires were synthesized by catalyst-free physical-vapor-deposition [33,34].

For the electric measurements, Keithley 6430 and Keithley 6487 source-meters were used. An Agilent N9310A signal generator was used to induce the electrical oscillations between the nanowires and the gold electrodes. The methodology for the resonance frequency and Q-factor measurements was similar to that previously reported [12,26].

Results and discussions

The schematics of an electrostatically actuated gate-less NEM switch in different OFF states can be seen in Figure 1a. The position of the flexile element (in our case nanowire) during the switch operation is determined by the resultant force arising from the superposition of an attractive electrical force $F(x,t)$ and a repulsive elastic force of the deflected from the equilibrium position nanowire $F_{elas}(x)$. The attractive force can be caused solely by an applied DC field between the electrodes, inducing deflection of the nanowire towards the opposite electrode or by the combination of

AC and DC fields, inducing the deflection and mechanical oscillations of the nanowire at its resonance frequency simultaneously.

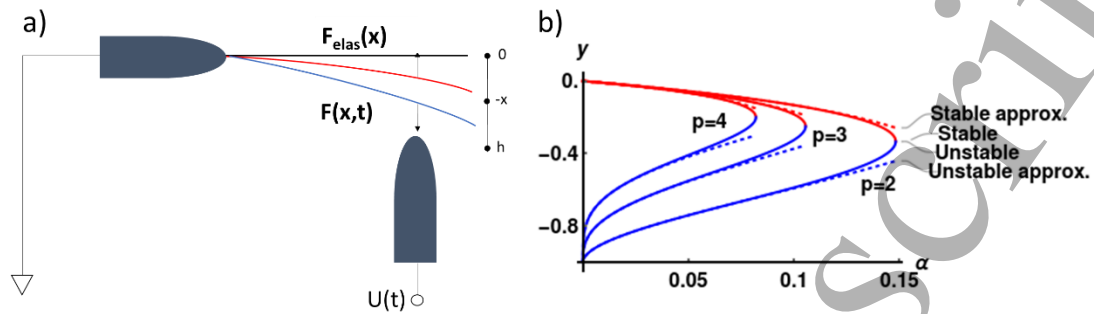


Figure 1. a) Electrostatically actuated NEM switch. $U(t)$ – voltage applied between the electrode and the flexile element, h – initial distance (gap) between the active element and the electrode, $-x$ – the deflection of the active element. Black line – initial position of the nanowire, when $U(t) = 0$. When $U(t)$ is applied, red line is the stable deflection of the nanowire and blue line is the unstable deflection of the nanowire, which leads to jump in contact or return to the stable position. b) Stable and unstable solutions of the equation 1. Numerical solution is given by the solid line, while approximation – by the dotted line. For each α there is a y value that represents the stable solution (red line) and the unstable solution (blue line) for the equation 4.

A theoretical model was developed to qualitatively describe the operation of this NEM switch. While not providing a quantitative description of the NEM switch operation, the model explains the main idea underlying the above configuration of the NEM switch, as well as illustrating the basic features of its operation.

Associating the coordinate x with the perpendicular deflection of the free end of the nanowire (Figure 1a), the differential equation corresponding to the motion of the nanowire is given by the expression shown in equation 1:

$$\ddot{x}(t) + \frac{2\pi f_0}{Q} \dot{x}(t) + (2\pi f_0)^2 x(t) = F(x, t), \quad (1)$$

where f_0 stands for the oscillator's material dependent mechanical eigen frequency of a nanowire, Q for its quality factor and $F(x,t)$ for the external electrostatic force per mass unit. This force is proportional to the square of the electric field. The latter is proportional to the voltage applied between the switching element and the counter electrode. If both DC and AC voltages are applied the resulting force $F(x,t)$ can be written as shown in equation 2:

$$F(x,t) = g(x) \left(U_{dc}^2 + \frac{1}{2} U_{ac}^2 + 2U_{dc}U_{ac}\sin(2\pi ft) - \frac{1}{2} U_{ac}^2 \cos(4\pi ft) \right), \quad (2)$$

where f is AC field frequency and U_{ac} , U_{dc} are AC and DC voltages – respectively.

The important feature of the force represented in equation 2 is that it depends not only on time directly, but also indirectly through the time-dependence on unknown function $g(x)$, as the coordinate x is also a function of time. An accurate enough model of the external force $F(x,t)$ can be obtained by solving the corresponding electrostatic problem (equation 2) numerically. In this paper we are interested only in the first mode of oscillation, which has the highest amplitude for oscillations, which permits the nanowire to be considered just as a harmonic oscillator. A simple qualitative consideration can then be used, together with an analytic model function, for $g(x)$ as shown in equation 3:

$$g(x) = \frac{-K}{(x+h)^p} \quad K > 0, p > 2 \quad (3)$$

The proportionality constant K , the power parameter p , and the distance between the initial non-deformed nanowire and the counter electrode surface h are present in equation 3. h is expected to be positive and x to be negative, thus the attractive

force grows when $x \rightarrow -h$. For simplicity a dimensionless coordinate $y = \frac{x}{h}$ will be used.

DC only

First, the static solution when only DC voltage was applied to the NEM switch [8–10,22] was considered to estimate the free parameters for the setup used in our experiments. In such a case, equation 1 reduces to equation 4 as shown below:

$$y = \frac{-\alpha}{(y+1)^p}; \alpha = K \frac{U_{dc}^2}{(2\pi f_0)^2}, \alpha_0 = \frac{K}{(2\pi f_0)^2}. \quad (4)$$

In Figure 1b, solutions to equation 4 in the interval $y \in [0;1]$ are plotted. For the case of $p=2$, by inspecting the roots of the corresponding cubic equation, if $\alpha < \frac{4}{27}$, two such solutions exist. The solution which corresponds to the smaller deflection (Figure 1 a,b red line) represents a stable equilibrium point. The solution which corresponds to the larger deflection (Figure 1a,b blue line) represents an unstable equilibrium from which a jump to contact can occur. The solution remains qualitatively unchanged if p is positive, which corresponds to all real experimental setups.

The approximate expression for the stable equilibrium (Figures 1a,b – dotted red line) can be found as a power expansion, shown in equation 5. To obtain this result one must represent the unknown function as a Taylor expansion around $\alpha = 0$. By taking derivatives of the equation (4) it is possible to get all of the necessary expansion coefficients, like $y(0) = 0, \frac{dy(0)}{d\alpha} = -1$, and so on.

$$y_{stable} = -\alpha - p\alpha^2 - \frac{1}{2}(p + 3p^2)\alpha^3 - \frac{1}{3}(p + 6p^2 + 8p^3)\alpha^4 + \dots \quad (5)$$

The approximate expression for the unstable equilibrium (Figures 1a,b – dashed blue line) can be written as detailed in equation 6. This result is achieved by rewriting the equation (4) as $y = -1 - \alpha^{1/p}/y^{1/p}$ and then expanding the unknown function in powers of $\alpha^{1/p}$ the same as it was done for the stable solution (5).

$$y_{unstable} = -1 + \alpha^{\frac{1}{p}} + \frac{1}{p}\alpha^{\frac{2}{p}} + \frac{3+p}{2p^2}\alpha^{\frac{3}{p}} + \frac{8+6p+p^2}{3p^3}\alpha^{\frac{4}{p}} + \dots \quad (6)$$

If the applied DC voltage increases, the parameter α which is proportional to the voltage squared (equation 4) also increases, and the nanowire will deflect more. When α reaches its largest value (Figure 1b – intersection between the blue and red lines), the jump-in voltage is reached, and the nanowire jumps into the contact with the electrode (Figure 1 a). The largest value of α depends on the chosen value of the parameter p . As can be seen from the Figure 1b, for $p = 3$ α is close to 0.105 and for $p=4$ α is close to 0.81.

To test the above theoretical model and to find the exact values of parameters p and α for our setup, the deflection of a GeSn nanowire as a function of applied voltage between the electrodes (Figure 2) was experimentally determined. The length of the GeSn nanowire was $L_{GeSn} = 14.8 \mu m$, radius $R_{GeSn} = 115 nm$, $f_0 = 623 kHz$, $Q = 550$ and the Young modulus $E = 106 GPa$. The initial separation gap h between the nanowire and the gold tip was $h = 0.57 \mu m$. From the Figure 2 it can be seen that the experimental points correspond well with the theoretical curve calculated for the parameters $\alpha_0 = \frac{K}{f_r^2} = (7.46 \pm 0.92) \cdot 10^{-4}$ and $p = 1.78 \pm 0.20$.

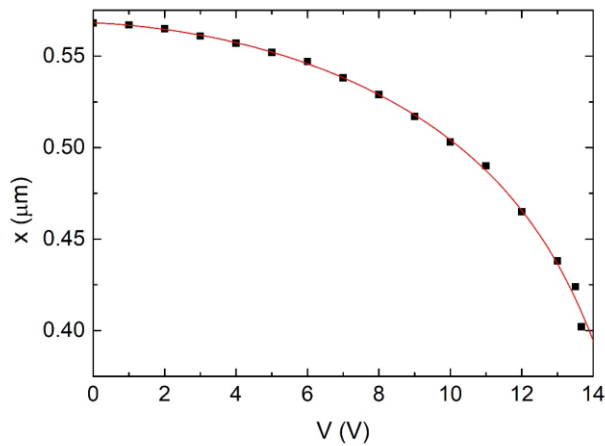


Figure 2 – Deflection of a GeSn nanowire with $L_{\text{GeSn}} = 14.8 \mu\text{m}$, $R_{\text{GeSn}} = 115 \text{ nm}$, $f_0 = 623 \text{ kHz}$, $Q = 550$ and $E = 106 \text{ GPa}$ as a function of static electric field applied between the NEM switch electrodes. Data points – experiment, red line – fitted theoretical calculations. After the last experimental point (13.7 V) the jump-in occurred at 13.8 V.

Figure 3 shows a DC-only driven gate-less NEM switch with a jump-in voltage of 13.8 V and jump-off voltage of 3.3 V. There is a hysteresis in the current when the voltage increases and decreases between 13.8 V and 20 V, which is not desirable for a NEM switch. The increased current in the reverse part of the I-V curve indicates that the switch elements may have been changed [29]. Repeated I-V measurements for another GeSn nanowire based device can be found in supplementary info (Figure 1 suppl.).

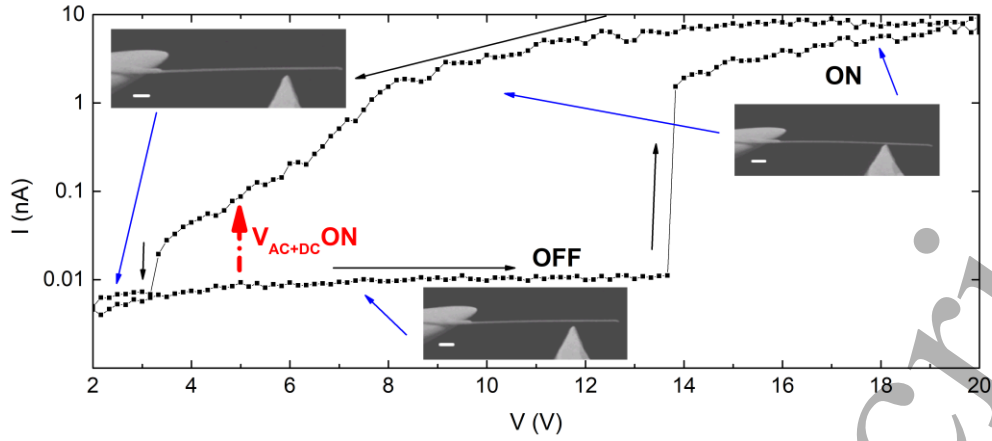


Figure 3 – I-V characteristics of a DC-only driven NEM switch for a GeSn nanowire with $L_{\text{GeSn}} = 14.8 \mu\text{m}$, $R_{\text{GeSn}} = 115 \text{ nm}$, $f_0 = 623 \text{ kHz}$, $Q = 550$ and $E = 106 \text{ GPa}$. Black arrows show direction of the voltage sweep. Blue arrows show SEM images of the NEM switch in ON and OFF states during the sweep. Red arrow represents the jump-in voltage for the switch driven by a combined AC-DC field. White scale bars in SEM pictures represent $1 \mu\text{m}$.

AC-DC combined

With all the experimental parameters for the theoretical model of a NEM switch acquired, the oscillations due to additionally applied AC voltage were considered.

To obtain the analytical expressions when both AC and DC voltages are applied between the NEM switch electrodes, the $g(y)$ function was approximated around its static solution y_0 as a linear function $g_{\text{approx}}(y)$, as shown in equation 7:

$$g_{\text{approx}}(y) = -K \left(\frac{1}{(y_0+1)^p} - \frac{p}{(y_0+1)^{p+1}} (y - y_0) \right) y_0 = y_{\text{stable}} \quad (7)$$

resulting in an equation of motion as shown in equation 8:

$$y''(t) + \frac{2\pi f_0}{Q} y'(t) + (2\pi f_U)^2 y(t) = (2\pi f_U)^2 y_0 + g_{\text{approx}}(y) \left(2U_{ac} U_{ac} \sin(2\pi f t) - \frac{1}{2} U_{ac}^2 \cos(4\pi f t) \right) \quad (2\pi f_U)^2 = (2\pi f_0)^2 - 2K \frac{(U_{ac}^2 + \frac{1}{2} U_{ac}^2)}{(y_0+1)^{p+1}} \quad (8)$$

Equation 8 clearly demonstrates that the resonance frequency f_U of the oscillator decreases under the influence of the electric field. This means that when a combined AC+DC field is applied between the switch electrodes, the resonance frequency f_U of the nanowire will be lower than its eigenfrequency f_0 . The solution to equation 8 can be obtained as an expansion in powers of U_{ac} . The linear term is presented in equation 9 below:

$$y = y_0 + y_1 U_{ac} + \dots y_1 = \frac{-2KU_{dc}}{(y_0+1)^p} (S \sin(2\pi f t) + C \cos(2\pi f t)) S = \frac{Q^2(f^2 - f_u^2)}{4\pi^2((f^2 - f_u^2)^2 Q^2 + (f f_0)^2)} C = \frac{Q(f f_0)}{4\pi^2((f^2 - f_u^2)^2 Q^2 + (f f_0)^2)} \quad (9)$$

The corresponding amplitude of the oscillations of the nanowire at any applied AC electric field frequency f is given by equation 10:

$$A = \frac{2KU_{dc}U_{ac}}{4\pi^2(y_0+1)^p \sqrt{(Q^2(f^2 - f_u^2)^2 + (f f_0)^2)}} \quad (10)$$

If this amplitude is larger than the difference between the unstable root, given in equation 6, and the stable root, given in the equation 5, then the jump-to-contact will occur. If the U_{ac} frequency f is equal to the field-modified resonance frequency f_u (equation 10) then the condition for jump-to-contact can be represented by equation 11:

$$U_{acJumpT} \geq \frac{(4\pi^2)^2 (f_u f_0)^2 (y_{stable}+1)^p (y_{stable} - y_{unstable})}{2KU_{dc}} \quad (11)$$

Equation 11 predicts that for our experimental setup with GeSn nanowire, where in a DC-only regime the jump-in voltage was 13.8 V, the combined AC+DC regime (with $U_{ACJumpT} = 0.15$ V at $f_U = 610.8$ kHz) will decrease the jump-in voltage down to $U_{dc} = 5$ V, which is almost a 3 times effective jump-in voltage reduction.

To prove the above assumption, an experiment with $U_{dc} = 5 \text{ V}$ and $f_U = 610.8 \text{ kHz}$ predicted by the theory was carried out with the same GeSn nanowire NEM device, but with a slightly larger $U_{AC} = 0.45 \text{ V}$ compared to the theoretical value of $U_{ACJumpT} = 0.15 \text{ V}$ (Figure 4a). A higher AC voltage than the theoretically predicted was chosen to achieve a stable switching of the NEM device; operating at the theoretical limit or close to it was undesirable due to possible instability (for example, thermal drift) of the experimental system.

In comparison to DC only switching, the lower combined AC+DC jump in voltage is shown in Figure 3 as a red arrow to emphasize the effect of the AC field on the jump in voltage. Such a reduction of the jump-in voltage may lead to a reduction of the current-induced effects and prolonged lifetime of the NEM switch ¹⁸.

The $I(t)$ characteristics of the subsequent switching for the same GeSn nanowire can be seen in Figure 4b. These characteristics indicate a clear ON-OFF behavior of the switch. The differences between the ON state current values most likely indicate some variations in the contact areas for each jump-in event. These differences may be due to the gold electrode which has a conic shape, and each time the cylindrical GeSn nanowire attaches in a slightly different position, thus changing the contact area. The demonstrated current switching can be used in biosensor applications where the signal is in picoampere range [36].

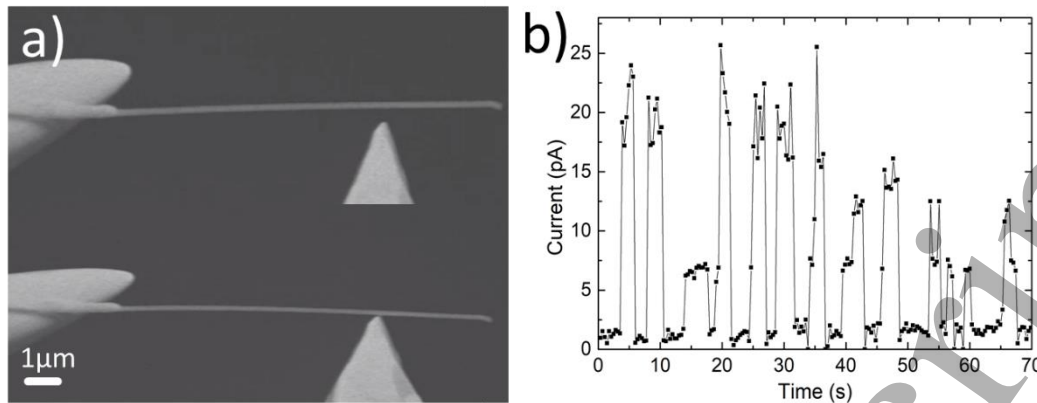


Figure 4 a) SEM images of the switching element - GeSn nanowire; b) $I(t)$ characteristics for combined AC+DC driven NEM switch. The different current values in ON states can be attributed to the different contact areas for each ON state.

To show our AC+DC method's applicability for the nanowires with different geometries, similar experiments were carried out for rectangular Bi_2Se_3 nanowires [33,34]. Due to their shape, resulting in a larger contact area and lower resistance [33,34], a higher current through the circuit could be achieved at the same voltage as for the cylindrical GeSn nanowires.

However, Bi_2Se_3 nanowires are prone to burn-out at much lower jump-in voltages [21] in comparison to Ge [8,22] and Si [9] nanowires, which makes them difficult to implement in electrostatically actuated NEM switches [21]. In our experimental setup, the Bi_2Se_3 nanowires switched ON-OFF in a combined AC+DC regime when $U_{ac} = 2.8 \text{ V}$ and $U_{dc} = 0.8 \text{ V}$ were applied between the switch electrodes (Figure 5a,b) respectively. After the AC+DC test was performed, it was not possible to test this nanowire in DC only regime in the same geometry, due to burning of the nanowire in jump-in when a $U_{dc} = 8.3 \text{ V}$ was applied. This fact confirms that the combined AC+DC

driven operation is promising for the NEM switches with flexile elements made of materials that cannot withstand high jump-in voltages.

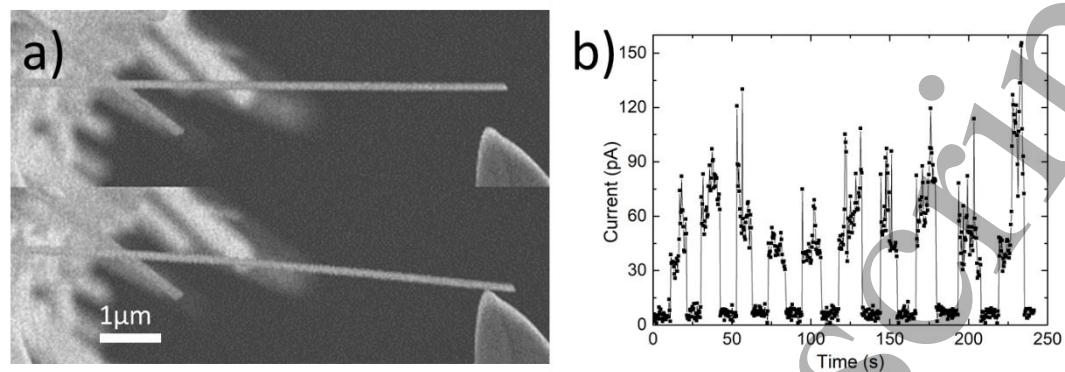


Figure 5 a) – SEM images of the NEM switch with Bi_2Se_3 flexile element in OFF and ON state; b) – $I(t)$ characteristics for this NEM switch.

Conclusions

We have demonstrated both theoretically and experimentally a novel method that implements both AC voltage, at the resonance frequency of nanowires, and DC voltage to decrease the jump in voltage for electrostatically actuated nanobeam-based NEM switches. We have shown experimentally that for GeSn nanowires used as a NEM switching element that the jump-in voltage can be reduced almost 3 times when operating in the AC+DC instead of DC-only regime. For Bi_2Se_3 nanowires the AC+DC method provided a low enough jump-in voltage to construct an operating switch that did not fail due to burn-out. Using combined AC+DC operating regimes is a convenient method to increase the durability of a NEM switch, by decreasing the impact due to such phenomena as electrostatic discharge, Joule heating, Fowler-Nordheim tunneling etc.

Acknowledgements.

This work was supported by ERDF project “Creation of nanoelectromechanical switches” (Project No.: 1.1.1.1/16/A/256) and Science Foundation Ireland (Project No.: 14/IA/2513).

References

- [1] Pisano A P 2007 MEMS and nano technology for the handheld, portable electronic and the automotive markets *TRANSDUCERS EUROSENSORS '07 - 4th Int. Conf. Solid-State Sensors, Actuators Microsystems* 1–3
- [2] George T 2002 MEMS/NEMS development for Space Applications at NASA/JPL Thomas ed J-C Chiao, V K Varadan and C Can² *Proc. SPIE* **4755** 556–67
- [3] Kaul A B 2012 *Microelectronics to Nanoelectronics: Materials, Devices & Manufacturability* (CRC Pr I Llc)
- [4] Feng X L, He R, Yang P and Roukes M L 2007 Very high frequency silicon nanowire electromechanical resonators *Nano Lett.* **7** 1953–9
- [5] Yang Y T, Callegari C, Feng X L, Ekin K L and Roukes M L 2006 Zeptogram-scale nanomechanical mass sensing *Nano Lett.* **6** 583–6
- [6] Hanay M S, Kelber S, Naik A K, Chi D, Hentz S, Bullard E C, Colinet E, Duraffourg L and Roukes M L 2012 Single-protein nanomechanical mass spectrometry in real time *Nat. Nanotechnol.* **7** 602–8
- [7] Kosmaka J, Andzane J, Prikulis J, Biswas S, Holmes J D and Erts D 2014 Application of a Nanoelectromechanical Mass Sensor for the Manipulation

- and Characterisation of Graphene and Graphite Flakes *Sci. Adv. Mater.* **6** 1–6
- [8] Andzane J, Petkov N, Livshits A I, Boland J J, Holmes J D and Erts D 2009 Two-Terminal nanoelectromechanical devices based on germanium nanowires *Nano Lett.* **9** 1824–9
- [9] Ziegler K J, Lyons D M, Holmes J D, Erts D, Polyakov B, Olin H, Svensson K and Olsson E 2004 Bistable nanoelectromechanical devices *Appl. Phys. Lett.* **84** 4074–6
- [10] Andzane J, Prikulis J, Dvorsek D, Mihailovic D and Erts D 2010 Two-terminal nanoelectromechanical bistable switches based on molybdenum-sulfur-iodine molecular wire bundles *Nanotechnology* **21** 1–7
- [11] Loh O Y and Espinosa H D 2012 Nanoelectromechanical contact switches *Nat. Nanotechnol.* **7** 283–95
- [12] Jasulaneca L, Kosmaca J, Meija R, Andzane J and Erts D 2018 Review: Electrostatically actuated nanobeam-based nanoelectromechanical switches – materials solutions and operational conditions *Beilstein J. Nanotechnol.* **9** 271–300
- [13] Yousif M Y A, Lundgren P, Ghavanini F, Enoksson P and Bengtsson S 2008 CMOS considerations in nanoelectromechanical carbon nanotube-based switches *Nanotechnology* **19** 271–300
- [14] Dadgour, F H and Banerjee K 2009 Hybrid NEMS–CMOS integrated circuits: a novel strategy for energy-efficient designs *IET Comput. Digit. Tech.* **3** 593
- [15] Lee J O, Song Y H, Kim M W, Kang M H, Oh J S, Yang H H and Yoon J B 2013 A

- sub-1-volt nanoelectromechanical switching device *Nat. Nanotechnol.* **8** 36–40
- [16] Li P, Jing G, Zhang B, Sando S and Cui T 2014 Single-crystalline monolayer and multilayer graphene nano switches *Appl. Phys. Lett.* **104** 113110
- [17] Sun J, Schmidt M E, Muruganathan M, Chong H M H and Mizuta H 2016 Large-scale nanoelectromechanical switches based on directly deposited nanocrystalline graphene on insulating substrates *Nanoscale* **8** 6659–65
- [18] Doelling C M, Kyle Vanderlick T, Song J and Srolovitz D 2007 Nanospot welding and contact evolution during cycling of a model microswitch *J. Appl. Phys.* **101** 1–7
- [19] Vincent M, Rowe S W, Poulain C, Mariolle D, Chiesi L, Houz F and Delamare J 2010 Field emission and material transfer in microswitches electrical contacts *Appl. Phys. Lett.* **97** 263503
- [20] Loh O, Wei X, Ke C, Sullivan J and Espinosa H D 2011 Robust carbon-nanotube-based nano-electromechanical devices: Understanding and eliminating prevalent failure modes using alternative electrode materials *Small* **7** 79–86
- [21] Kosmaca J, Andzane J, Baitimirova M, Lombardi F and Erts D 2016 Role of Nanoelectromechanical Switching in the Operation of Nanostructured Bi₂Se₃ Interlayers between Conductive Electrodes *ACS Appl. Mater. Interfaces* **8** 12257–62
- [22] Andzane J, Priekulis J, Meija R, Kosmaca J, Biswas S, Holmes J D and Erts D 2013 Application of Ge nanowire for two-input bistable nanoelectromechanical

- switch *Medziagotyra* **19** 254–7
- [23] Jang W W, Lee J M J O J M, Yoon J B, Kim M S, Lee J M J O J M, Kim S M, Cho K H, Kim D W, Park D and Lee W S 2008 Fabrication and characterization of a nanoelectromechanical switch with 15-nm -thick suspension air gap *Appl. Phys. Lett.* **92** 103110
- [24] Lee J O, Kim M W, Ko S D, Kang H O, Bae W H, Kang M H, Kim K N, Yoo D E and Yoon J B 2009 3-Terminal nanoelectromechanical switching device in insulating liquid media for low voltage operation and reliability improvement *Tech. Dig. - Int. Electron Devices Meet. IEDM* 227–30
- [25] Ngo L T, Almécija D, Sader J E, Daly B, Petkov N, Holmes J D, Erts D and Boland J J 2006 Ultimate-strength germanium nanowires *Nano Lett.* **6** 2964–8
- [26] Kosmaca J, Jasulaneca L, Meija R, Andzane J, Romanova M, Kunakova G and Erts D 2017 Young's modulus and indirect morphological analysis of Bi₂Se₃ nanoribbons by resonance measurements *Nanotechnology* **28** 325701
- [27] Livshits A I, Jasulaneca L, Kosmaca J, Meija R, Holmes J D and Erts D 2017 Extra tension at electrode-nanowire adhesive contacts in nano-electromechanical devices *Eur. J. Mech. A/Solids* **66** 412–22
- [28] Andzane J, Meija R, Livshits A I, Prikulis J, Biswas S, Holmes J D and Erts D 2013 An AC-assisted single-nanowire electromechanical switch *J. Mater. Chem. C* **1** 7134–8
- [29] Meija R, Kosmaca J, Jasulaneca L, Petersons K, Biswas S, Holmes J D and Erts D 2015 Electric current induced modification of germanium nanowire NEM

- switch contact *Nanotechnology* **26** 195503
- [30] Kosmaka J, Meija R, Antsov M, Kunakova G, Sondors R, Sjomkane M, Iatsunskiy I, Coy E, Doherty J, Biswas S, Holmes J D and Erts D 2019 Effect of tapering on mechanical and electrical properties of GeSn alloy nanowires *Submitted*
- [31] Sistani M, Seifner M S, Bartmann M G, Smoliner J, Lugstein A and Barth S 2018 Electrical characterization and examination of temperature-induced degradation of metastable Ge 0.81 Sn 0.19 nanowires *Nanoscale* **10** 19443–9
- [32] Biswas S, Doherty J, Saladukha D, Ramasse Q, Majumdar D, Upmanyu M, Singha A, Ochalski T, Morris M A and Holmes J D 2016 Non-equilibrium induction of tin in germanium: Towards direct bandgap Ge 1-xSn_x nanowires *Nat. Commun.* **7** 11405
- [33] Andzane J, Kunakova G, Charpentier S, Hrkac V, Kienle L, Baitimirova M, Bauch T, Lombardi F and Erts D 2015 Catalyst-free vapour-solid technique for deposition of Bi₂Te₃ and Bi₂Se₃ nanowires/nanobelts with topological insulator properties *Nanoscale* **7** 15935–44
- [34] Kunakova G, Galletti L, Charpentier S, Andzane J, Erts D, Léonard F, Spataru C D, Bauch T and Lombardi F 2018 Bulk-Free Topological Insulator Bi₂Se₃ nanoribbons with Magnetotransport Signatures of Dirac Surface States *Nanoscale* **10** 19595–602
- [35] Mishra S K, Satpathy S and Jespen O 1997 Electronic structure and thermoelectric properties of bismuth telluride and bismuth selenide *J. Phys.*

Condens. Matter **9** 461–70

- [36] Vidal J C, Bonel L, Ezquerro A, Hernández S, Bertolín J R, Cubel C and Castillo J R 2013 Electrochemical affinity biosensors for detection of mycotoxins: A review *Biosens. Bioelectron.* **49** 146–58